A Study on Integration of Wave Energy Converter and Semi-submersible Floating Wind Turbine: A Water Tank Test

Hongzhong Zhu[#1], Changhong Hu[*2], Makoto Sueyoshi[*2], Shigeo Yoshida[*2]
[#]Research and Education Center for Green Technology, Kyushu University
6-1 Kasugakouen, Kasuga, Fukuoka 816-8580, JAPAN
[1]zhuhongzhong@riam.kyushu-u.ac.jp
[*]Research Institute for Applied Mechanics, Kyushu University
6-1 Kasugakouen, Kasuga, Fukuoka 816-8580, JAPAN
[2]hu,sueyoshi,yoshidas@riam.kyushu-u.ac.jp

***Abstract*—Economic efficiency and structural reliability are strongly required for ocean energy exploration. The integration of wave energy converter and floating offshore wind turbine has the potential to reduce the cost of energy since they can share the mooring system and the infrastructure of power grid. In this study, oscillating-water-column-type wave energy converters mounted on a semisubmersible-type floating wind turbine are considered. The wave energy converter is designed not only to capture wave energy but also to work as a damper of the semisubmersible for helping on enhancing the fatigue life of the wind turbine. Controllers for the wave energy converter and wind turbine for reducing the pitch motion of the semisubmersible are also presented in the study. The experimental results illustrate that the pitch of semisubmersible can be reduced by the controllers in most of the cases. However, the effectiveness of the controllers could be limited by the capacity of the wave energy converter especially when the motion of the floating turbine is large.**

***Keywords*—Wave energy converter, semi-submersible floating wind turbine, semi-active control, water tank test.**

I. Introduction

Countries around the world are putting substantial effort on the development of wind energy technologies for decarbonization. In 2016, wind power generated about 4% of global electricity while its capacity shows steady expansion [1]. The International Energy Agency (IEA) targets 15% to 18% share of global electricity from wind power by 2050 in its roadmap, which will avoid emissions of up to 4.8 gigatonnes (Gt) of carbon dioxide (CO_2) per year [2]. Offshore wind energy is recognized as an important component part for addressing the targets owing to the fact that the significant wind resources are available over the oceans.

The sustainable development of the offshore wind energy requires reliable floating platforms. Although platforms are usually designed with good sea-keeping performance and good stability, environmental forces induced by wind, waves and ocean currents can, however, induce undesired heave and pitch motion, which would induce large external loads on structure and reduce the fatigue life of devices on the platforms [3, 4, 5]. Suzuki and Sato have performed some pioneering work on investigating the effects of motion of floating platform on the strength of offshore wind turbine blades, and they come to the result that pitching with amplitude of 5 degrees will lead to a 50% increase of sectional modulus of a blade to avoid fatigue failure. Hence, motion suppression of the floating platform is a very important issue in many practical situations [6]. Although the floating platforms are designed with sophisticated analysis, Huijs *et al.* have reported that the maximum inclination of the floaters would also reach to 10 degrees according to model tests [7]. In order to further reduce the motions, various methods and state-of-art structures were proposed in the literature. In [8] and [9], novel water-entrapment plates with large horizontal skirts were designed to increase the added-mass and viscous loads to semi-submersible platform. In the methods, the natural periods of the platform in heave, pitch and roll are adjusted to avoid the resonance with the environmental forces. Though the water-entrapment plates can be systematically designed considering strength analysis and fatigue loads, the fabrication cost and maintenance, however, would limit its applications. In addition, Roddier and Cermelli proposed an interesting concept of structure consisting of three column tubes which are partly filled with water [10]. The water can be pumped between the three columns to balance out the environment forces. A major advantage of the concept is that the platform pitch motion can be controlled by pumping the water from some columns to the others. However, the response may be too slow to non-regular waves in addition to the requirement of external power supply.

Although the ocean waves are the primary source causing the floater motion, it is also a type of renewable energy resource with high power density [11]. The global gross theoretical resource is estimated at about 3.7 TW, a quantity that is comparable with the world's present power consumption. The technologies on utilization of wave energy for electricity production are not yet mature. A number of demonstration projects exists, but these are generally still in the R&D phase and the cost of the energy from these installations are multiple times greater than the target (market) level [12].

Various technologies, such as oscillating water columns [13], wave activated bodies [14], and overtopping [15] are applied with fixed structure or floating structure. Recent studies also put effort in combining wave energy converters (WEC) with floating offshore wind turbine (FOWT) for a better utilization of marine space and lower installation cost owing to the shared electrical grid connections and mooring systems [16, 17, 18, 19]. Though there are many advantages, the combination also introduces the inter-influence between WEC and FOWT that makes the whole system complex. Perez and Iglesias have reported that particular attention should be paid to the wind turbine foundation affected by the installation of the WEC since the inclination of foundation may exceed the design limit [20]. Development of a device which can not only extract energy from wave but also help on reducing the platform motion attracts authors' attention. A conceptual design that treats a WEC as a suspension system for the floating platform has been proposed and the parameters of WEC are designed based on mathematical optimization method [21]. However, the realization of the concept requires more carefully studies.

This study develops an experimental model on evaluating the integration of WECs and floating wind turbine. Firstly, the design aspects of the system are introduced. The characteristics of the system and the wave energy conversion efficiency are then investigated. The effectiveness of the controllers and their limitation are finally explored.

II. Design Aspects

The experimental system consists of a semisubmersible with mooring system, a wind turbine mounted on the semisubmersible, and three wave energy converters installed at the vertices of the platform. The detailed design are expressed as follows.

A. Wind Turbine

A pitch-regulated wind turbine with upwind design is applied for this study. The rotor of the wind turbine is remodelled from a helicopter (model: FORZA 450EX) with the rotor diameter 720 mm. The rotation speed of the wind turbine is controlled by an electronic speed controller (ESC) by a feed-forward manner. The minimum rotation speed, which is measured as 1400 rpm without the incident wind, is applied in the experiment. The blades are no tapered and no twisted blades with a symmetric airfoil (the chord length is 26 mm and the thickness is 3 mm). The blade pitch is controlled by a swashplate via three digital servo motors. The tower is mounted on the semisubmersible by a tripod. The hub of the wind turbine is located at 550 mm above the platform. The mass of the wind turbine is 0.61 kg and the center of mass is about 480 mm above the platform along the centerline of the tower.

B. Semisubmersible and Mooring System

The semisubmersible is a triangular-shaped platform made of acrylic resin. It consists of three hollow cylinders, three pontoons between the cylinders and the plates to strengthen the structure. Three hollow cylinders with outer diameter 250 mm and thickness 5 mm, which are reserved for installing the wave energy converters, are placed at the vertices of the platform. The three pontoons with outer diameter 80 mm and thickness 5 mm are applied to connect the hollow cylinders and provide the primary buoyancy for the system. Some square columns made of Styrofoam are mounted on the platform to adjust the water plane area of the semisubmersible. The Computer Aided Design (CAD) model of semisubmersible is shown in Fig. 1. The properties of the semisubmersible are listed in Table I. The edge length of the platform, say, the distance between the cylinders, is 0.95 m. The metacenter of the floating wind turbine is 146 mm. This experimental semisubmersible is expected to be a 1:200 scale of platform for a 10 MW floating wind turbine.

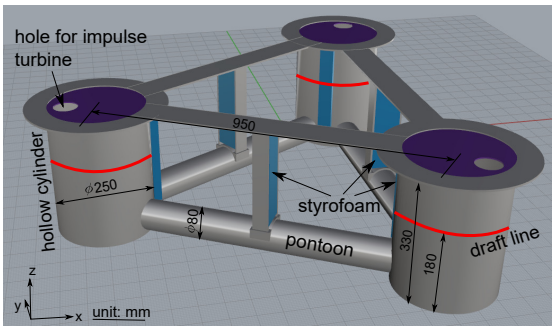

Fig. 1. CAD model of the semisubmersible.

TABLE I
Properties of Semisubmersible

Property	Value
Floater draft (mm)	180
Displacement (mm^3)	1.44×10^7
Elevation of platform (mm)	150*
Floater mass (kg)	12.24
Center of buoyancy (mm)	-124*
Center of mass (mm)	-79*
Moment of inertia (Ix,Iy,Iz) (kgm^2)	(1.45, 1.45, 2.15)

* The values are with respect to the undisturbed water surface.

Preliminary numerical studies of the system indicate that the motion amplitudes of the semisubmersible caused by the incident waves are small in the experimental water tank conditions. Therefore, a simple linear spring system with stiffness 0.08 N/mm is used in the experiment to approximate the anchor-chain mooring system. The mooring lines are connected to the outer wall of the hollow cylinders with an angle of 30 deg away from the centerline of the cylinders.

C. Wave Energy Converter

Oscillating-water-column type wave energy converters are applied in this study. The schematic view of the wave energy converter is shown in Fig. 2. A self-rectifying impulse turbine with fixed twin guide vane at the both sides of the turbine rotor is applied as the power-take-off (PTO). The rotor radius

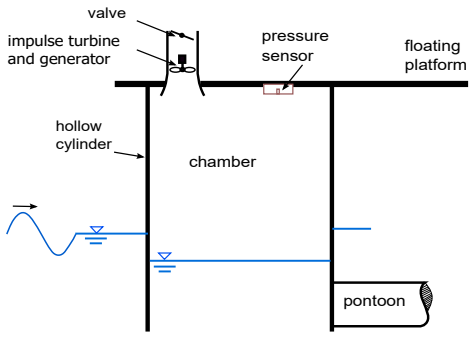

Fig. 2. Schematic of wave energy converter.

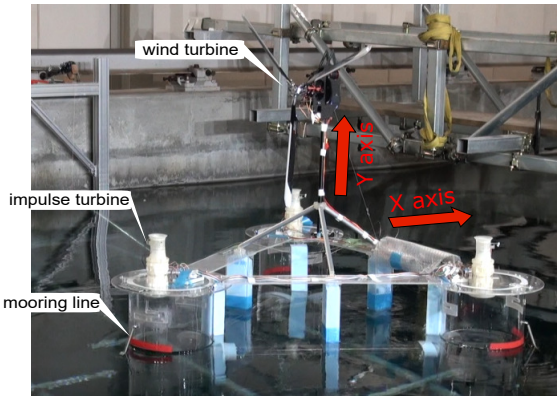

Fig. 3. Model for water tank test.

of the impulse turbine is 30 mm and the length of rotor blade is 8.5 mm. A brushed DC machine is applied as the generator. The fluctuation of the water surface forces the air to flow in/out of the chamber to drive the impulse turbine and the generator.

A valve is applied at the outlet of the well turbine in order to regulate the air flowing in/out of the chamber, so as to control the water surface in the hollow cylinder and to influence the motion of the platform. A digital servo motor is applied to control the valve for its compact and fast response. An air pressure sensor (Adafruit BME280) is set at the top of the chamber to measure the pressure of the chamber and to provide the necessary information for the controller.

The model based on the aforementioned design is shown in Fig. 3. For ease of explanation, the origin of the body coordinate system is located on the undisturbed free surface beneath the tower. The x axis is in wind direction and z axis points upward normal to the water surface. The y axis is chosen to coincide with the right-hand rule.

D. Control System

Control system is designed for the valves of the wave energy converters and the blades of the wind turbine in order to reduce the pitch motion of the platform. As the initial step of the study, the controllers are designed separately so that the cooperative control between the valves of the WECs and the blade pitch is not discussed.

1) Controller for valves: Two-state Sky-Hook Control method [22] is applied to control the valves of the wave energy converters based on the air pressure in the chamber and the gyro angular velocity of the platform. For the valve of the WEC at the upwind side of the semisubmersible, the control law is set by

$$\begin{cases} g_y P_f > 0, & \text{valve=open,} \\ g_y P_f \leq 0, & \text{valve=close,} \end{cases} \tag{1}$$

where g_y is the pitch angular velocity of the platform, P_f is the gauge pressure in the chamber. The valve is open to let the air flow in/out of the chamber to reduce the conjunction level between the water surface in the cylinder and the platform. In this way, the air in the chamber is not trapped and the air-induced force on the platform is minimum. On the contrary, the valve is close and the air-induced force can provide a resistant term to help on reducing the platform pitch motion. The valves in the downwind side of the platform are controlled in the same way that

$$\begin{cases} g_y P_r > 0, & \text{valve=close,} \\ g_y P_r \leq 0, & \text{valve=open,} \end{cases} \tag{2}$$

where P_r is the gauge pressure in the downwind chambers.

2) Blade pitch control for platform motion reduction: Control of blade pitch angle for power regulation is skipped since it is not the topic of this study. Blade pitch control presented in this paper aims to reduce the platform motion. The pitch motion of the floating wind turbine can be modelled approximately as a second-order system as

$$J\dot{g}_y + Dg_y + K\theta = M + \Delta M, \tag{3}$$

where θ is the pitch angle, J is the moment of inertia of the floating wind turbine, D is the damping term, and K is the restoring coefficient. The moment M is the combination of hydrodynamics, mooring force and rotor thrust. ΔM represents the additional moment caused by blade pitch action. The coefficient K can be calculated based on metacenter and second moment of water plane area. The damping effect can be increased if ΔM is proportional to $-g_y$ expressed by

$$\Delta M = -D_a g_y, \tag{4}$$

where D_a is the additional damping coefficient. The additional moment caused by the blade pitch can be expressed by

$$\Delta M = \frac{\partial F_t}{\partial \beta} \Delta \beta H, \tag{5}$$

where H is the hub height, F_t is the thrust force formulated by

$$F_t = \frac{1}{2} \rho_a A C_t(\lambda, \beta) V^2. \tag{6}$$

Here, ρ_a is the air density, A is the rotor area, V is the wind speed. The thrust coefficient C_t, which is the function of the tip-speed ratio λ and pitch angle β, is calculated from blade element momentum (BEM) theory [23]. The coefficient C_t with $\lambda = 10$, which is the equilibrium operation point of the

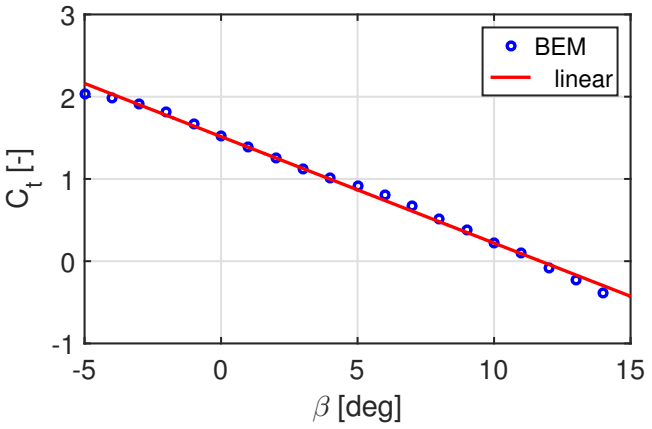

Fig. 4. Thrust coefficient by BEM and the linear approximation at tip-speed ratio $\lambda = 10$.

wind turbine in the experiment, is shown as a function of blade pitch angle in Fig. 4.

From (4) and (5), the control law for the blade pitch on motion reduction is given by

$$\Delta\beta = \frac{-D_a g_y}{\frac{\partial F_t}{\partial \beta} H} = 2\frac{-D_a g_y}{\rho_a A V^2 H \frac{\partial C_t}{\partial \beta}}. \tag{7}$$

Linear approximation is applied and the partial derivative of C_t with respect to β is about $\frac{\partial C_t}{\partial \beta} = -0.12$.

A computer-on-module (Intel® Edison Kit for Arduino) is applied for implementing the control algorithm. A 9-axis motion tracking device (MPU 9150) is mounted on the platform to measure the pitching angular velocity of the platform. The pressure in the chambers of the WECs and the motion information of the platform are sent to the module by Inter-Integrated-Circuit (I2C) method. A first-order low-pass filter with the bandwidth of 2 Hz is applied to improve the signal-to-noise ratio (SNR) of the measured signals. The control period is set as 0.1 s considering the measurement delay of the sensors (including the signal transmission and signal processing) and the response of the digital servo motors.

III. Results

The model experiment is carried out in the water tank with length 65 m, width 5 m and depth 7 m at the Research Institute for Applied Mechanics (RIAM) of Kyushu University. A wind generator with 12 axial flow fans is installed on the tank, and it is able to generate a maximum wind speed of 5 m/s. A movable seafloor frame is installed in the water at the depth 0.9 m to set the mooring system. A high-speed digital video camera is applied to measure the motion of the floating wind turbine. In the experiment, wind and waves travel in the same direction along the positive x-axis.

Free decay experiment is carried out to measure the characteristics of the floating wind turbine with wave energy converters. The valves of the wave energy converters are set to open, and the results in time series are shown in Fig. 5. Owing to the symmetry of the platform, the free decay motion

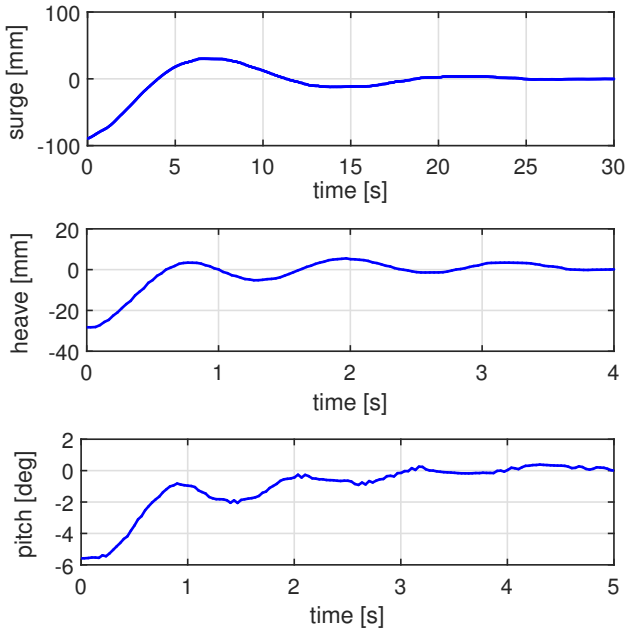

Fig. 5. Free decay motion of the floating wind turbine in surge (upper graph), heave (middle graph) and pitch (lower graph).

TABLE II
Natural periods (coupled) of the floating wind turbine.

surge	heave	pitch
14.0 s	1.20 s	1.16 s

in surge, heave and pitch is investigated only. The natural frequencies of the motion are list in Table II. Owing to the WECs that the air cannot freely flow in/out of the chamber, the natural periods of the heave and pitch of the full scale system (scaled using Froude scaling method) are smaller than the common semisubmersible-type floating wind turbine discussed in [24].

Then, the energy conversion efficiency of the wave energy converters and the effectiveness of the controllers on platform pitch motion reduction are evaluated. The wind speed is set as $V = 5$ m/s so that the wind turbine operates with tip-speed-ratio of $\lambda = 10$ and nominal blade pitch angle $\beta_0 = 5$ deg. The wave period and wave height for experiment are listed in Table III. The ratio of the wave length to the diameter of hollow cylinder Λ/D and the ratio of the wave length to the edge length of floating platform Λ/L are also given in the Table.

To evaluate the wave energy conversion efficiency of the WECs, the valves of the WECs are fully opened and the controller of the valves is inactive. Owing to the fact that the impulse turbines cannot rotate stably so as the generator voltage during the experiment, the primary energy calculated from the air flowing in/out of the chamber is applied for

TABLE III
EXPERIMENTAL CONDITIONS

case	wave period [s]	wave height [cm]	Λ/D	Λ/L
1	0.90	1.25	5	1.32
2	1.13	2.00	8	2.11
3	1.39	2.00	12	3.16
4	1.60	2.67	16	4.21
5	1.79	2.50	20	5.26
6	2.00	3.13	25	6.58
7	2.19	3.75	30	7.90

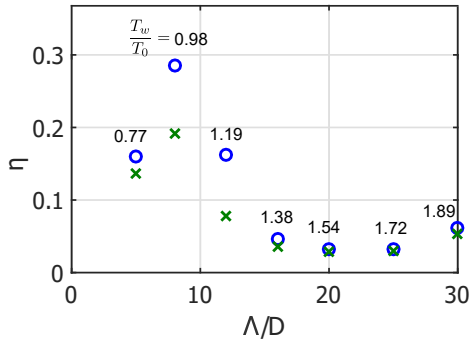

Fig. 6. Primary wave energy conversion efficiency of the WECs without wind turbine operation ('O' mark) and with wind turbine operation ('×' mark). The ratio of the wave period to the pitch natural period of the floating wind turbine $\frac{T_w}{T_0}$ is also specified.

evaluation. The flow rate of the air is estimated by

$$Q = CA_s\sqrt{\frac{2|P|}{\rho_a}}, \tag{8}$$

where C is the flow coefficient to be set as $C = 0.8$, A_s is the cross-section area of the impulse turbine, P is the gauge pressure of the chamber and ρ_a is the air density. The energy extracted from the wave by one WEC is calculated by

$$E_a = \int_0^T |P|Qdt, \tag{9}$$

where T is the time span of experiment. Therefore, the primary conversion efficiency is

$$\eta = \frac{E_{a_f} + 2E_{a_r}}{E_w}. \tag{10}$$

E_{a_f} is the energy extracted by the front cylinder and E_{a_r} is the energy extracted by a rear cylinder. E_w is the wave energy covered by the three cylinders calculated by

$$E_w = \left\{\frac{\rho_w g^2 \zeta_0^2}{8\pi} T_w 3D \left(1 + \frac{2kh}{\sinh 2kh}\right) \tanh kh\right\} T, \tag{11}$$

where ρ_w is the water density, g the gravitational acceleration, ζ_0 the wave amplitude, T_w the wave period, k the wave number, h the water depth and D the diameter of the hollow cylinders. The primary energy conversion efficiency of WECs without wind turbine operation and with wind turbine

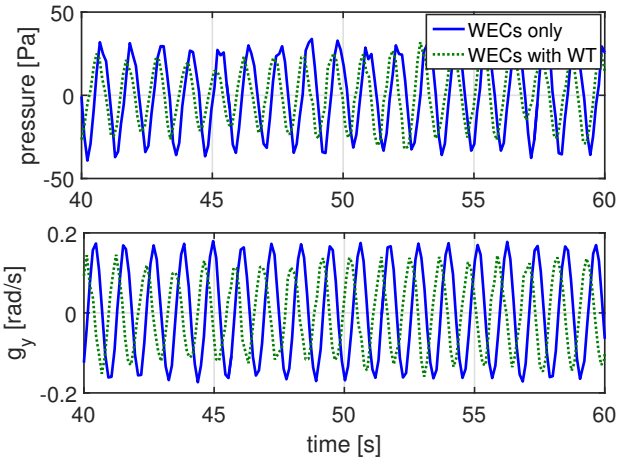

Fig. 7. The air pressure (upper graph) of the front chamber and the pitch motion of the platform (lower graph) of case 2. The solid lines show the results when WECs operate without wind turbine and the dotted line show the results when WECs and wind turbine are under operation together.

operation is shown in Fig. 6. It is observed that best wave energy conversion efficiency is obtained when the wave period is close to the natural period of the pitch motion of the floating platform. In addition, owing to the air damping effect at the rotor plane when the wind turbine is under operation, the motion of the platform is suppressed and the power conversion efficiency is reduced, as it can be seen in Fig. 6 that efficiency represented by '×'-mark is lower than 'o'-mark. The air pressure in the front chamber and the pitching angular velocity of the platform in case 2 are illustrated in Fig. 7. When the wind turbine is under operation, not only the platform motion, but also the air pressure in the chambers is reduced.

Finally, the controller of the valves of WECs and the controller of the blade pitch are activated to investigate the effectiveness on motion reduction. The platform pitch reduction ratio used for evaluation is defined by

$$\text{pitch reduction ratio} = \frac{\Theta_{\text{w/o ctrl}} - \Theta_{\text{w/ ctrl}}}{\Theta_{\text{w/o ctrl}}}, \tag{12}$$

where $\Theta_{\text{w/o ctrl}}$ is the fundamental amplitude of pitch motion without control and $\Theta_{\text{w/ ctrl}}$ is the fundamental amplitude of pitch motion with control. Similarly, the cases that the wind turbine is in parked condition and the cases that the wind turbine is under operation are discussed, and the results are shown in Fig. 8 and Fig. 9. In the figures, the upper graphs show the pitch amplitude without/with control and the lower graphs show the pitch reduction ratio. From Fig. 8, it can be found that the platform pitch motion is reduced in all of the cases when the controller of the valves of WECs is activated. However, the motion reduction ratio varies inversely with the motion amplitude. The reduction ratio is small (about 5%) when the motion amplitude is large (case 2 and case 3) and better motion reduction is obtained in small motion. The capacity limitation of the WECs may be the primary reason for the phenomenon.

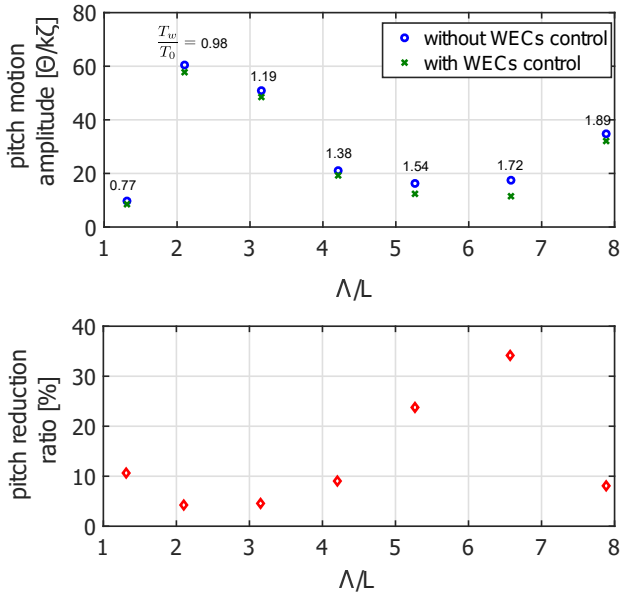

Fig. 8. The results of the floating platform pitch when the wind turbine is in parked condition. In the upper graph, the 'o'-mark shows the results without WECs control and the '×'-mark shows the results with WECs control. The ratio of the wave period to the pitch natural period of the floating wind turbine $\frac{T_w}{T_0}$ is also specified. The ratio of pitch reduction by WECs control is in lower graph.

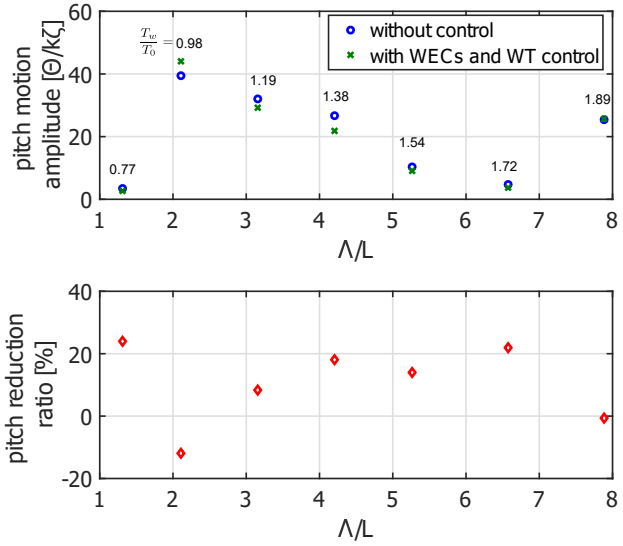

Fig. 9. The results of the floating platform pitch when the wind turbine is under operation. In the upper graph, the 'o'-mark shows the results without WECs control and the '×'-mark shows the results with WECs control. The ratio of the wave period to the pitch natural period of the floating wind turbine $\frac{T_w}{T_0}$ is also specified. The ratio of pitch reduction by WECs control is in lower graph.

When the wind turbine is under operation, the platform pitch motion can be reduced by the controllers in most of the cases, as shown in Fig. 9. Similarly, the motion reduction ratio is better when the platform motion amplitude is small. However, the platform motion in case 2 is augmented when the controllers are activated. The blade pitch control (7) without considering the change of rotor rotation speed would be the main reason of the deterioration. The large platform pitch motion induces large change of blade pitch, which causes the change of the rotor rotation speed since the rotor speed is not regulated by feedback loop. In addition, the control of WECs and the control of blade pitch of wind turbine may cause inter-influence since they are designed separately. Therefore, sophisticated cooperative control taking into account of the real-time rotation speed and pitch angle and air pressure in the chambers is necessary for this study. The issue is considered to be addressed in our future work.

IV. Conclusion and Future Work

A study on integration of semisubmersible-type floating wind turbine and oscillating-water-column-type wave energy converters is performed based on water tank test. The wave energy converters are implemented to capture wave induced energy as well as to reduce the pitch motion of floating platform. The structure design and the controllers for platform motion reduction are presented. Although the design of the integration system is still a big challenge, some important items can be concluded from this study:

- Design of wave energy converter should take into account of the characteristics of the semisubmersible, since the motion of the semisubmersible would significantly affect the wave energy conversion efficiency. The wave energy converter would reduce the natural periods of the floating wind turbine, which need to be considered seriously.
- A semisubmersible is usually designed with small motion to prevent the wind turbine. However, high efficiency of wave energy conversion requires large motion of platform. Instead of pursuing the wave energy conversion efficiency, increase of damping effect or help on reducing the wave exciting force on semisubmersible would be the primary consideration of the wave energy converter for the integration.
- Cooperative control between the wave energy converters and the blade pitch of wind turbine should be considered for platform motion reduction. Control with insufficient information may deteriorate the system performance.

In addition, two-state Sky-Hook control leads to large valves motion and sharp change of air pressure in chambers. Therefore, a more sophisticated controller is required for practical situation. The small scale of the wave energy converters and the mechanical friction cause the well turbines not to work smoothly, and the total wave energy conversion efficiency cannot be properly evaluated. The above problems will be considered in our next study.

Acknowledgment

This research was partially supported by JSPS KAKENHI Grant Number 17K14616.

References

[1] IEA., "Renewables 2017," http://www.iea.org, 2017, [accessed on 26/April/2018].

[2] ——, "Technology roadmap: Wind energy-2013 edition," http://www.iea.org, 2013, [accessed on 26/April/2018].

[3] T. Ishihara, P. Phuc, H. Sukegawa, K. Shimada, and T. Ohyama, "A study on the dynamic response of a semi-submersible floating offshore wind turbine system part 1: A water tank test," in *Proceedings of the 12th International Conference on Wind Engineering*, 2007, pp. 2511–2518.

[4] A. R. Henderson and M. H. Patel, "On the modelling of a floating offshore wind turbine," *Wind Energy*, vol. 6, no. 1, pp. 53–86, 2003.

[5] O. Faltinsen, *Sea Loads on Ships and Offshore Structures*. Cambridge: Cambridge University Press, 1993.

[6] H. Suzuki and A. Sato, "Load on turbine blade induced by motion of floating platform and design requirement for the platform," in *Proceedings of the 26th International Conference on Offshore Mechanics and Arctic Engineering*, 2007, pp. 519–525.

[7] F. Huijs, J. Mikx, F. Savenije, and E.-J. de Ridder, "Integrated design of floater, mooring and control system for a semi-submersible floating wind turbine," in *EWEA Offshore 2013 Vienna*, Vienna, 2013.

[8] A. Aubault, C. Cermelli, and D. Roddier, "Structural design of a semi-submersible platform with water-entrapment plates based on a time-domain hydrodynamic algorithm coupled with finite-elements," in *Proceedings of 6th International Offshore and Polar Engineering Conference*, San Francisco, 2006, pp. 187–194.

[9] H. Zhu, J. Ou, and G. Zhai, "Conceptual design of a deep draft semi-submersible platform with a movable heave-plate," *Journal of Ocean University of China*, vol. 11, no. 1, pp. 7–12, 2012.

[10] D. Roddier and C. Cermelli, "Column-stabilized offshore platform with water-entrapment plates and asymmetric mooring system for support of offshore wind turbines," patent, US008471396B2, 2013.

[11] J. Falnes, "A review of wave-energy extraction," *Marine structures*, vol. 20, no. 4, pp. 185–201, 2007.

[12] A. Pecher and J. P. Kofoed, *Handbook of Ocean Wave Energy*. Springer, 2017.

[13] A. F. Falcão and J. C. Henriques, "Oscillating-water-column wave energy converters and air turbines: A review," *Renewable Energy*, vol. 85, pp. 1391–1424, 2016.

[14] A. Ghasemi, M. Anbarsooz, A. Malvandi, A. Ghasemi, and F. Hedayati, "A nonlinear computational modeling of wave energy converters: A tethered point absorber and a bottom-hinged flap device," *Renewable energy*, vol. 103, pp. 774–785, 2017.

[15] J. P. Kofoed, P. Frigaard, E. Friis-Madsen, and H. C. Sørensen, "Prototype testing of the wave energy converter wave dragon," *Renewable energy*, vol. 31, no. 2, pp. 181–189, 2006.

[16] M. Borg, M. Collu, and F. P. Brennan, "Use of a wave energy converter as a motion suppression device for floating wind turbines," *Energy Procedia*, vol. 35, pp. 223–233, 2013.

[17] S. Chandrasekaran, D. Raphel, and S. Shree, "Deep ocean wave energy systems: experimental investigations," *Journal of Naval Architecture and Marine Engineering*, vol. 11, no. 2, pp. 139–146, 2014.

[18] C. Perez, D. Greaves, and G. Iglesias, "A review of combined wave and offshore wind energy," *Renewable and Sustainable Energy Reviews*, vol. 42, pp. 141–153, 2015.

[19] L. Li, Y. Gao, Z. Yuan, S. Day, and Z. Hu, "Dynamic response and power production of a floating integrated wind, wave and tidal energy system," *Renewable Energy*, vol. 116, pp. 412–422, 2018.

[20] C. Perez and G. Iglesias, "Integration of wave energy converters and offshore windmills," in *Proceedings of the fourth international conference on ocean energy (ICOE)*, Dublin, Ireland, 2012.

[21] H. Zhu, C. Hu, and Y. Liu, "Optimum design of a passive suspension system of a semisubmersible for pitching reduction," *Journal of Dynamic Systems, Measurement, and Control*, vol. 138, no. 12, p. 121003, 2016.

[22] R. Williams, "Automotive active suspensions part 2: practical considerations," *Proceedings of the Institution of Mechanical Engineers, Part D: Journal of Automobile Engineering*, vol. 211, no. 6, pp. 427–444, 1997.

[23] S. A. Ning, "A simple solution method for the blade element momentum equations with guaranteed convergence," *Wind Energy*, vol. 17, no. 9, pp. 1327–1345, 2014.

[24] M. Karimirad and C. Michailides, "V-shaped semisubmersible offshore wind turbine: An alternative concept for offshore wind technology," *Renewable Energy*, vol. 83, pp. 126–143, 2015.